

Figure S1. SLC15A4 is not required for mast-cell differentiation

(A) Peritoneal mast cells were collected from naïve WT or *Slc15a4*^{-/-} mice by peritoneal lavage and were analyzed by flow cytometry. (B) Tissue resident mast cells in the ear of WT or *Slc15a4*^{-/-} mice. Mast cells were visualized by Toluidine blue staining. Number of mast cells in the area of the ear of WT (n=4) or *Slc15a4*^{-/-} (n=5) mice was counted. n.s.: not significant. (C) Proliferation of WT and *Slc15a4*^{-/-} BMMCs. EdU uptake by BMMCs stimulated by IL-3 or SCF, analyzed by flow cytometry. (D, E) Expression of mast-cell proteases at the message (D) or protein level (E) in BMMCs. The cDNA from WT or *Slc15a4*^{-/-} BMMCs was subjected to quantitative RT-PCR for *Mcpt4*, *Mcpt5*, *Mcpt6*, *Cpa3*, and *Hrh4*. The whole-cell lysates of WT or *Slc15a4*^{-/-} BMMCs were immunoblotted to determine the CPA3 and mMCP5 (Chymase) levels. **P*<0.05. (F) Levels of enzymes for serotonin synthesis in WT or *Slc15a4*^{-/-} BMMCs, analyzed by quantitative RT-PCR.

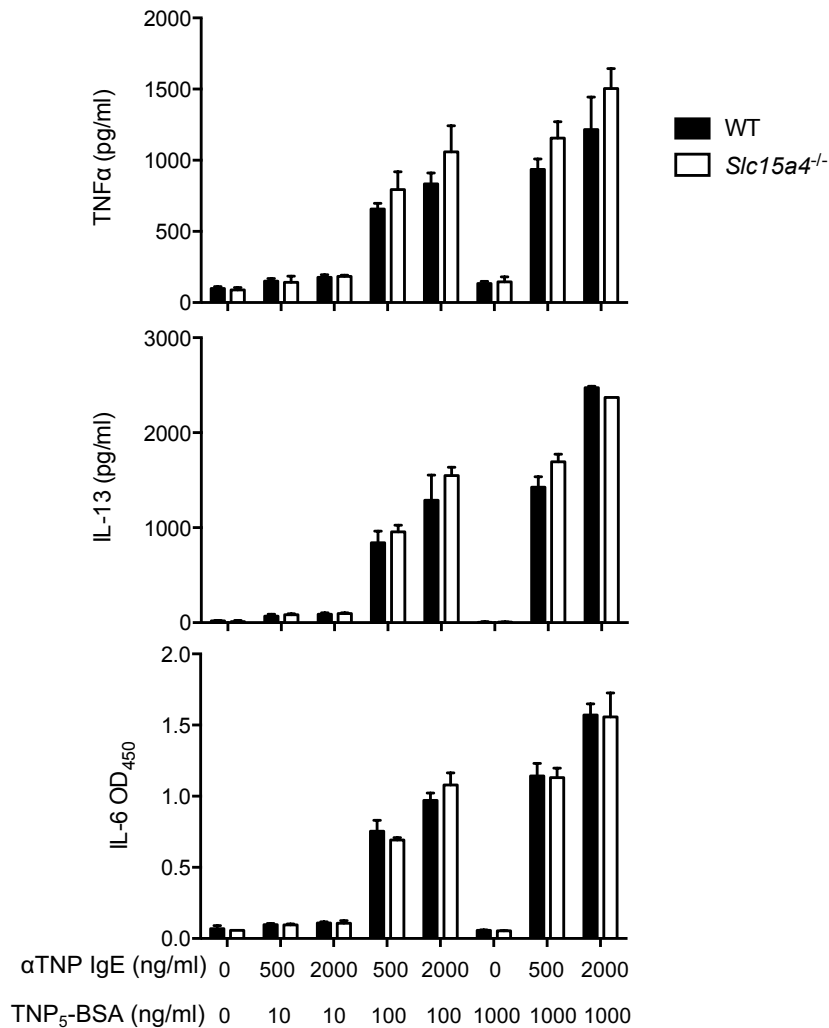


Figure S2. Cytokine response to FcεRI ligation is not influenced by the dose of anti-IgE or TNP-BSA.

WT or *Slc15a4*^{-/-} BMDCs were sensitized with anti-TNP IgE at the indicated concentrations overnight and then stimulated with TNP₅-BSA at the indicated concentrations for 6 h. TNFα, IL-13, and IL-6 levels in the culture supernatant were assessed by ELISA.

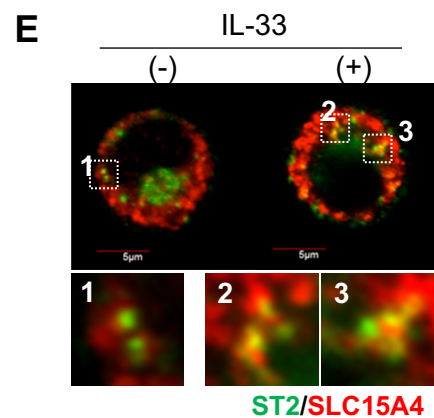
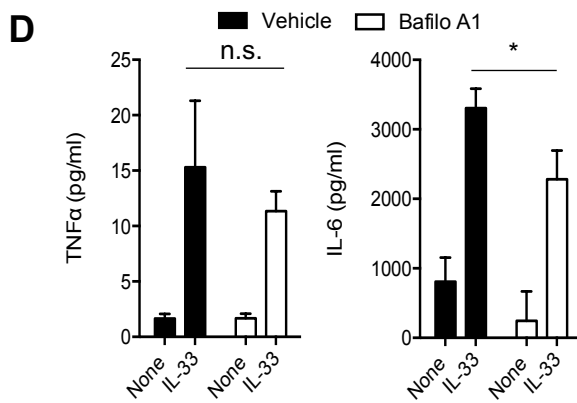
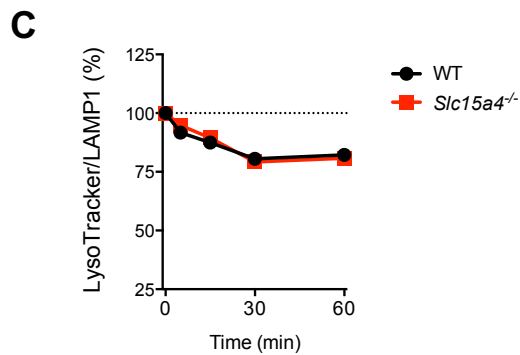
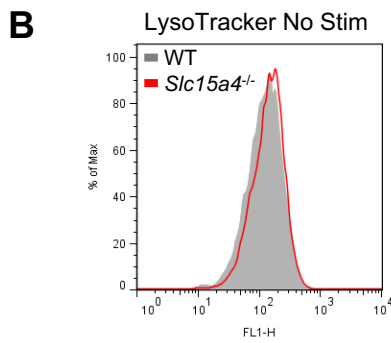
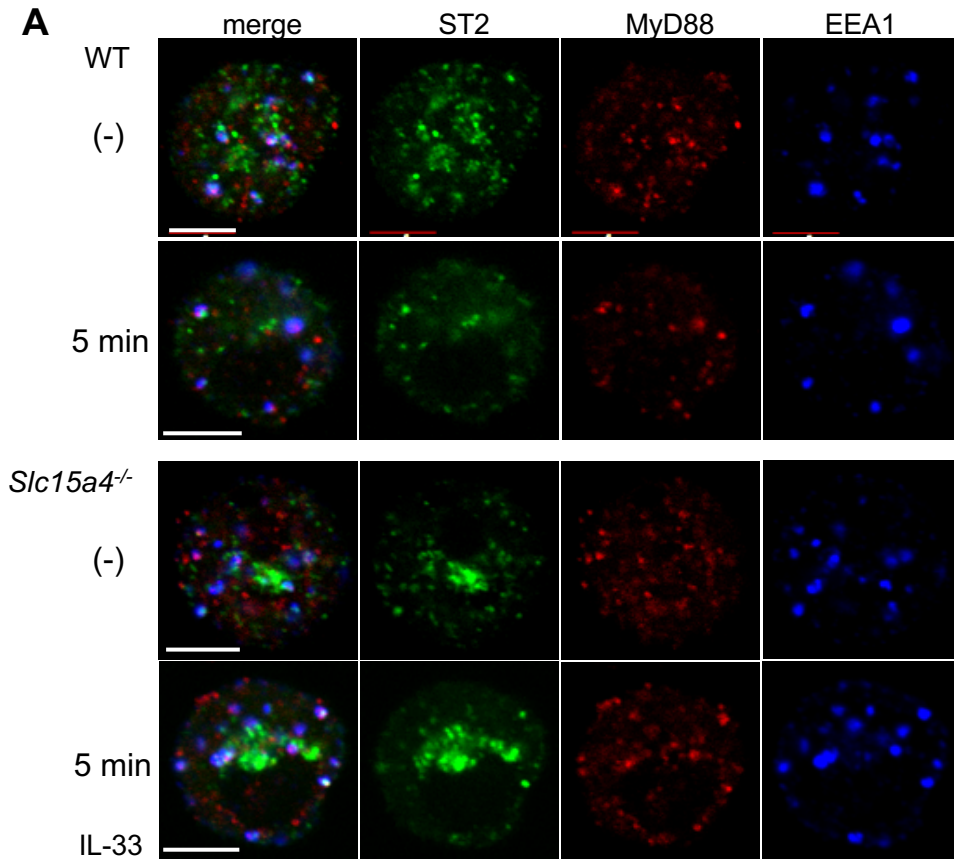


Figure S3.

The subcellular distribution of IL-33R α (ST2) and MyD88 upon IL-33 stimulation.

(A) Quantitative comparison of acidic compartments between WT and *Slc15a4*^{-/-} BMMCs. LysoTracker fluorescence in WT or *Slc15a4*^{-/-} BMMCs was quantified by flow cytometry. (B) LysoTracker fluorescence after IL-33 stimulation. WT or *Slc15a4*^{-/-} BMMCs were stimulated with recombinant IL-33 for the indicated periods, and cells were stained with LysoTracker Green or were fixed, permeabilized, and stained with anti-LAMP1. Fluorescence was quantified by flow cytometry. (C) Impact of endosomal acidification blockade on the IL-33 response in BMMCs. WT BMMCs treated with Bafilomycin A1 were stimulated with recombinant IL-33 for 6 h. Cytokine levels in the culture supernatant were determined by ELISA. * $P < 0.05$. (D) Colocalization of SLC15A4 and ST2 IL-33 receptors in mast cells. Hematopoietic-cell-derived mast cells expressing HA-tagged human SLC15A4, unstimulated or stimulated with recombinant IL-33 for 5 min, were analyzed under a confocal microscope. ST2 and SLC15A4 subcellular localization was detected with anti-ST2 and anti-HA monoclonal antibodies and visualized by confocal microscopy.

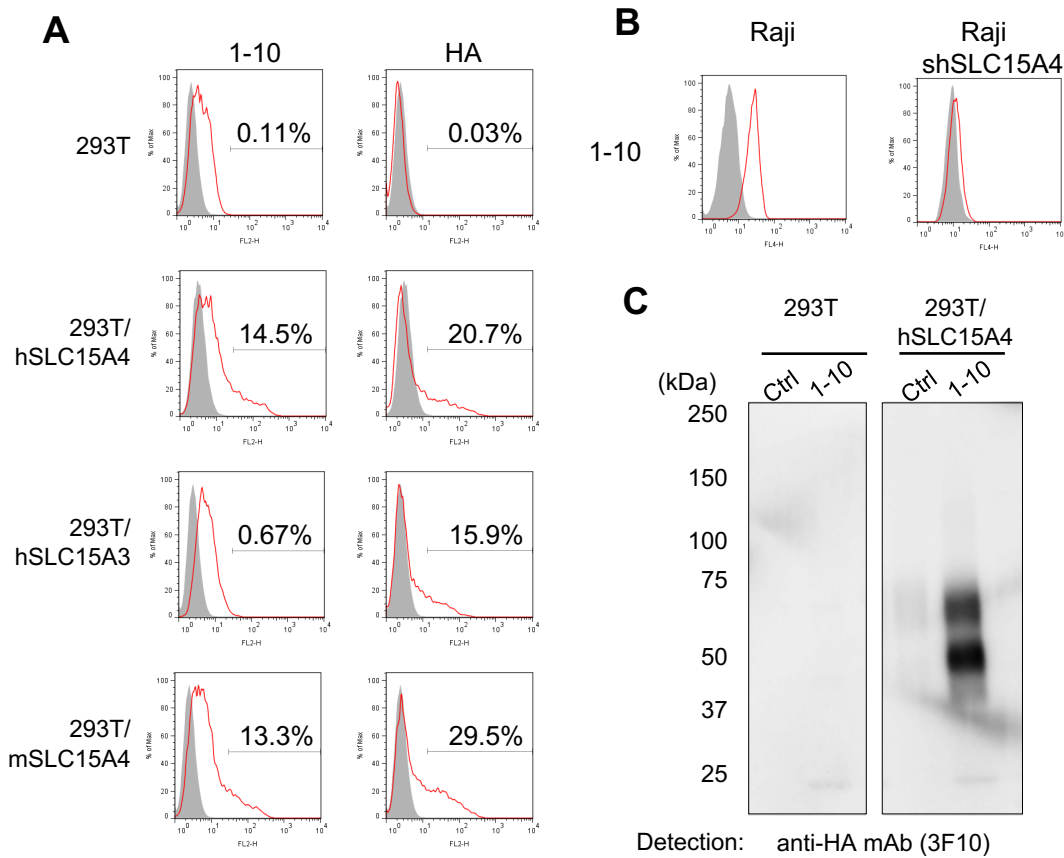


Figure S4. Characterization of the anti-SLC15A4 monoclonal antibody (mAb) clone 1-10.

(A) Antigen specificity of the clone 1-10 mAb was analyzed by flow cytometry with intracellular staining of HEK293T cells expressing human SLC15A4, human SLC15A3, or mouse SLC15A4. Fixed and permeabilized cells were stained with the 1-10 mAb in combination with PE-conjugated anti-mouse IgG. (B) SLC15A4 levels in Raji cells. Control or *SLC15A4*-silenced Raji cells were stained with the 1-10 mAb in combination with AlexaFluor647-conjugated anti-mouse IgG, and fluorescence was quantified by flow cytometry. (C) Biochemical analysis of the 1-10 mAb. SLC15A4 was immunoprecipitated with the 1-10 mAb. Lysates of control HEK293T cells or cells expressing the HA-tagged human SLC15A4 were pulled down with the 1-10 mAb, and the precipitated protein was detected by immunoblotting with the anti-HA antibody.

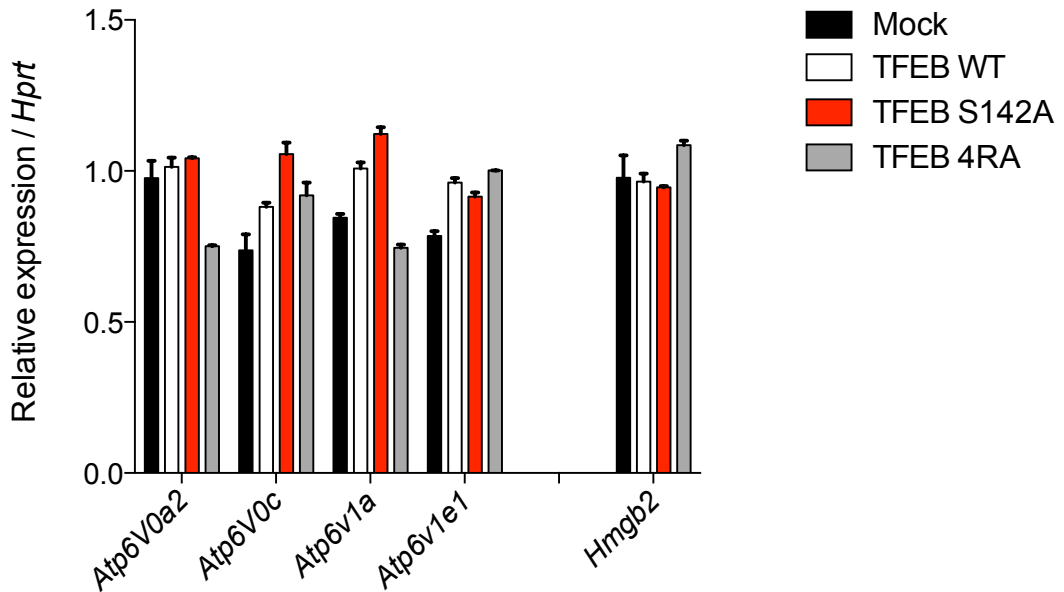


Figure S5. Expression of other lysosome-associated genes in RBL2H3 cells expressing human TFEB mutants.

The cDNA from RBL2H3 transfectants was subjected to quantitative RT-PCR. *Hmgb2* was used as a control.

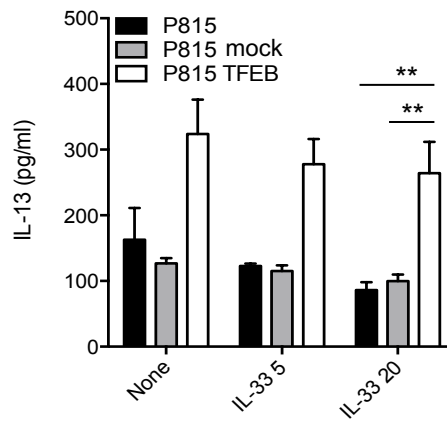


Figure S6. IL-13 levels in the culture supernatant of P815 transfectants stimulated with recombinant IL-33 for 24 h. ****** $P < 0.01$.